APPLYING CONVENTIONAL VEGETATION VIGOR INDICES TO UAS-DERIVED ORTHOMOSAICS: ISSUES AND CONSIDERATIONS

Klaas Pauly

Trimble Navigation Ltd.
Ghent, Belgium

ABSTRACT

In recent years, unmanned airborne systems (UAS) have gained a lot of interest for their potential use in precision agriculture. While the imagery from color infrared (CIR)-enabled commercial off-the-shelf cameras onboard UAS is appealing to facilitate crop scouting, the application of quantitative spectral analyses is influenced by a range of confounding factors. In contrast to satellite (and conventional airborne) imagery, typical UAS datasets are (1) subject to unknown and highly varying irradiance due to the ability to fly in all weather conditions at all times of the day, (2) using uncalibrated sensors and compressed and distorted digital numbers, preventing conversion to reflectance factors in an efficient and broadly applicable way, and (3) characterized by a very high spatial resolution causing a significant amount of soil and shadow noise to be visible at the sub-canopy level. When directly applying vegetation vigor indices (such as the NDVI) that have been historically designed to work using reflectance factors derived from satellite imagery at the canopy level and at a much coarser resolution than UAS imagery, these characteristics may compromise the validity of the resulting maps. While it is clear that calibrated algorithms are needed to produce maps that need a high level of confidence for decision making and prescription mapping, we recognize the need for simple crop scouting strategies based on automated and out-of-the-box data gathering practices to identify problem areas in a field, prior to more in-depth analytical approaches, which can be applied later after crop scouting has been done using the simpler approach. Here, we visualize the effects described above on a realistic scenario, and quantify the influences of soil and shadow noise on relative, uncalibrated vegetation vigor indices, using a Trimble UX5 UAS equipped with different filters. The multiple band combinations obtained in this way allow the calculation of several vegetation vigor index maps, which are then evaluated against handheld Trimble GreenSeeker NDVI measurements. Our goal is to describe potential pitfalls in using only a relative NDVI based on default UAS-based imagery for crop scouting, and to suggest ways to increase our understanding of UAS-based imagery for crop scouting.

Keywords: UAS, Trimble UX5, crop scouting, NDVI, remote sensing

INTRODUCTION

Worldwide, the adoption of precision agriculture techniques in order to increase land productivity is rising sharply, with more than 30% of US Mid-western famers estimated to use some form of precision farming to date (Mulla, 2013). Most notably, the advent of remote and proximal sensing techniques has enabled service providers and crop growers to get the relevant data for adjusting management practices from the field zonal level down to a grid cell level in a timely manner. Although the spatial, spectral as well as temporal resolution of conventional (satellite and airborne) remote sensing products has dramatically increased lately, getting visible color and near-infrared (NIR) imagery is inherently limited to cloud-free conditions for the field at the time of overpass. In humid regions, this can result in the inability to get remote sensing data on crucial days around seeding, plant emergence, early growth stages, and before harvesting. Additionally, the cost per hectare is often prohibitively expensive for relatively small farms or agronomists managing several fields scattered across a relatively small area. On the other hand, driving sensor-equipped tractors across entire fields for the sole purpose of mapping can be a time consuming and expensive process and is not always desirable because of potential damage to crops and soil. Moreover, gathering several variables such as different vegetation vigor index (VVI) maps and dense soil or crop surface models using proximal sensing only may require several sensor setups. Also, proximal active optical sensors tend to monitor only the upper parts of a canopy of vegetation due to the loss of spectral irradiance over the distance from the sensor to various depths of the canopy.

In recent years, autonomous unmanned aircraft systems (UAS) have gained a lot of interest as a tool in between proximal and conventional remote sensing to deal with the drawbacks of both approaches in gathering timely information on the current state of fields, both before and after plant emergence. Besides multirotor platforms that have the ability to carry heavy imaging payloads such as multispectral or even hyperspectral cameras to do detailed spot analyses and to identify specific causes for growth issues, initial field and crop scouting is often done using a small and fast-flying fixed wing UAS (typically up to 1 m wide and weighing in at less than 3 kg). These typically allow mapping of intra-field variability of areas around 500 ha using a commercial, off-the-shelf very high resolution visible color camera, often modified to capture the NIR in addition to some of the visible colors (known as color infrared, CIR), in a highly automated workflow from flight planning to image processing. Next to the ability of delivering a georeferenced visible or false color orthomosaic on the same day or overnight at resolutions out of reach for spaceborne and conventional airborne mapping (2.5 – 15 cm ground sample distance, GSD), the inherent photogrammetric generation of a dense crop surface or bare terrain model with pixel-level accuracy during image processing of UAS imagery is a significant added advantage compared to other remote or proximal sensing techniques.

Although regulations imposed on the commercial exploitation of this emerging technology are still notoriously stringent in some countries (most notably the US), the ease-of-use and relatively affordable cost (especially in highly frequent use) have led to forecasts estimating more than 82 billion USD economic impact of UAS in agriculture in the first decade after commercial airspace integration in the

US alone, with around 80% of the total commercial UAS market devoted to precision agriculture (West, 2014).

Regardless of the obvious advantages of UAS as a data gathering tool to overcome some of the issues related to conventional proximal and remote sensing, some difficulties remain with the quality of the collected imagery and the interpretation of these images that have been obtained from commercial cameras mounted on UAS, primarily in the quantitative analysis of spectral signals for leaf chlorophyll-related N assessments, variable rate prescription mapping, and yield forecasting. In fact, while recent advances in image processing algorithms have solved issues such as the orthorectification of the imagery, some of the biggest advantages of UAS also directly result in the biggest difficulties in the quantitative analysis of the imagery. First, the ability (and the resulting common practice) of flying over a field of interest in a diverse range of weather and light conditions on different times of the day, causes the spectral irradiances to vary greatly between and even within flight datasets, as opposed to satellites revisiting an area at a specific time of the day, and covering vast areas under the same irradiance conditions at once. Even for cloudless conditions over fields of interest, the very high resolution imagery also includes small shadows and dark soil patches in between leaves that are not resolved in the GSDs associated with satellite imagery and that may confound spectral analyses. The overall reflectance of a canopy is affected by these shadows and patterns of bright and dark soils, especially for NIR wavelengths where leaves are quite translucent. Next, the off-the-shelf commercial cameras used in UAS often lack any radiometric and spectral sensor calibration in an absolute sense. Furthermore, since all of the RGB Bayer pixel filters on the sensor are sensitive to a certain part of the red-edge (RE) and NIR radiation as well, all visible color band digital numbers (DNs) in CIR imagery are affected by out-of-band radiation to a certain extent, making it difficult to get pure spectra from a single flight. Moreover, to facilitate fast data handling, the use of in-camera (unspecified) gamma correction and the use of 8-bit JPEG compression of imagery (as opposed to using image sensor data in 14-bit uncompressed linear RAW format) is common practice. Lastly, non-linear blending algorithms are commonly implemented during the mosaicking of orthorectified images. While this makes the mosaics visually appealing and free of obvious seam lines, the radiometric qualities may be affected. The latter factors cause the linear relationship between reflectances of surface materials and digital data to be lost, and prevent the conventional conversion of pixel DNs to reflectance factors used in physically calibrated remote sensing algorithms. Efforts such as mounting an irradiance sensor on the UAS or using spectral calibration panels and measurements in the fields can have their merit, but are typically very expensive, time consuming, and not always applicable (e.g. under rapidly moving clouds).

Although many vegetation vigor indices were originally designed to work on linear, uncompressed DNs or even reflectance factors and give meaningful values at the canopy level (such as the NDVI), most UAS-based research has continued to use (only) out-of-camera JPEG DNs to calculate these indices on very high resolution imagery including sub-canopy features. Some studies were able to show that the influence of the JPEG compression in quantitative analyses can be rather limited in some specific cases of UAS-based mapping (Lebourgeois et al.,

2008; Lelong et al., 2008), although these findings cannot be generalized. The apparent ease of use with which JPEG DNs, blended into a seamless orthomosaic, can be plugged into the NDVI, has led to a large number of studies relying mainly, if not only, on the so-called relative NDVI calculated in this way to reveal contrasts in crop fields and to find out where vegetation vigor is clearly affected. Success has varied (Hunt et al., 2010; Lebourgeois et al., 2012; Zhang and Kovacs, 2012).

While we highly recommend that actual prescription mapping for decision making and variable rate application should be done based on calibrated spectral algorithms, we do also recognize the need for easy, automated crop scouting based on compressed out-of-camera UAS data and common image processing algorithms to pinpoint issues in fields prior to more in-depth analyses. However, due to the difference in the data characteristics for which conventional vegetation vigor indices were designed, as opposed to the data characteristics on which the indices are applied, the unassuming use of only a relative NDVI may lead to entirely unwarranted conclusions, as a number of factors significantly influence the resulting values.

The goal of this study is to identify some of these factors, demonstrate them on real data resulting from day-to-day UAS operations, and to present ways in which the reliability of relative (uncalibrated) VVI maps for crop scouting based on out-of-camera imagery may be improved. Ultimately, we want to raise awareness on the pitfalls in the use of only a relative NDVI for decision making and to simply suggest alternative approaches, rather than claiming a definitive way to get highly accurate results based on data that are inherently prone to a number of spectrally confounding factors.

MATERIALS AND METHODS

Test site, image acquisition and field data

The flight area consists of farmland located in Assenede, Belgium, at approximately 51.23° N, 3.78° E, comprising 1 km of fields with barley, winter and summer wheat, potato, maize, grass and some cover crops, all managed under uniform application regimes.

Flights were executed using the Trimble UX5 UAS, a 2.5 kg electrically driven fixed wing platform with a wingspan of 1 m, capable of flying fully automated from launch to landing in winds of up to 18 m s^{-1} and light rainfall while covering up to 2 km at 3 cm GSD in a 50 min flight. The camera used for agricultural projects with the Trimble UX5 is a modified Sony NEX-5T from which the internal NIR-blocking filter has been replaced by transparent glass. With a pixel pitch of 4.8 µm, the 16 megapixel (MP) APS-C format sensor ensures a very high dynamic range and signal-to-noise ratio with the ability to store imagery in 14-bit linear uncompressed RAW alongside 8-bit JPEG, although in this study only JPEG imagery was used to reflect the common practice of UAS-based crop scouting. The acquisition of different visible and NIR band combinations during different flights using the same camera is possible through the use of external bandpass filters that can be placed in the standard screw mount

filter holder in the bottom of the UX5 airframe. In order to make the best decisions for this study, the best cut-on and cut-off wavelengths for filters were determined based on a spectral response analysis of the camera using a monochromator with the camera set to JPEG (fig. 1), as response curves vary significantly between JPEG and RAW.

Two seasons were covered by the flights: a late winter flight on 19 Mar. 2014 and a late spring flight on 28 May 2014 covering the same central area. Meteorological conditions differed for both flights, with no cloud cover and low solar elevation angles during the winter flight and heavy cloud cover with light rain during the spring flight. Each flight was planned at 100 m above ground level resulting in around 750 images per flight at 3 cm GSD. On each day, imagery was acquired in R(b1):G(b2):B(b3) using a Schneider Optics 486 UV/NIR blocking filter (passing 380 – 700 nm), and R(b1):G(b2):NIR(b3) obtained by a Schneider Optics 040 orange filter (with a cut-on at 530 nm, blocking all blue light). Additionally, on 28 May NIR(b1):G(b2) imagery was also acquired using a Schneider Optics IF 062 green filter (passing 490 – 580 nm and above 780 nm). Since the blue band (b3) appeared to have the highest sensitivity to the NIR (> 800 nm) and the 040 orange filter blocks out all visible light to which the blue pixels are sensitive, this band was consequently used as the NIR band for the RGNIR imagery. However, as the 062 green filter still transmits some visible light in the sensitivity range of the blue pixels, but all red light and the red edge are effectively blocked out by the filter, the red band (b1) of the NIRG imagery was used as the NIR band.

In order to compare the UAS data to another commonly accepted form of crop scouting, field verification data on vegetation vigor were collected by walking across the fields with a handheld Trimble GreenSeeker and georeferenced with centimeter level accuracy using a Trimble R8 RTK GNSS.

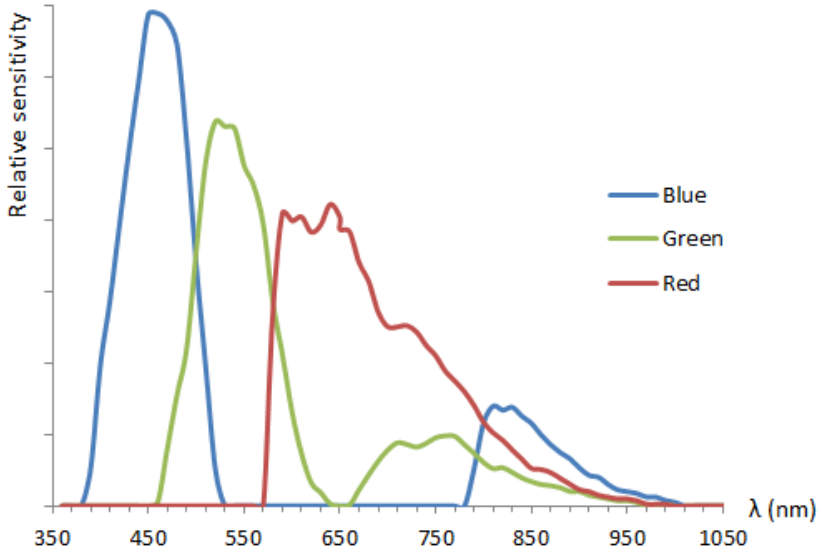

Figure 1. Relative spectral response of the full spectrum modified Sony NEX-5T onboard the Trimble UX5 in JPEG mode.

This resulted in 75 and 120 point measurements on each day, respectively, comprising all relevant terrain types from bare soil over juvenile plants to dense canopy cover for the different species. In order to get an NDVI reading over a circular patch to facilitate digitizing on raster imagery, the GreenSeeker was triggered during a circular sweeping motion resulting in a circular coverage with a radius of 16 cm on the crop canopy level for which the average NDVI value was noted.

Image processing

Out-of-camera JPEG imagery was processed in the usual workflow with the fully automated Trimble Business Center Aerial Photogrammetry Module (TBC APM), generating a dense colored point cloud and an orthomosaic at 3 cm GSD. At least 5 ground control points (GCPs) measured with a Trimble R8 RTK GNSS were used to process each dataset to ensure pixel-level alignment of the different orthomosaics, and to make sure GreenSeeker measurements were plotted on the correct pixels. At least 10 additional points per dataset were not used during processing in order to serve as independent accuracy check points.

Image analysis

All analyses were carried out in ESRI ArcGIS 10.2. Table 1 summarizes the VVI maps that were extracted from the orthomosaics for each day. In addition to the well-known conventional vegetation indices, we chose to include an alternative approach in the form of principal components analysis (PCA). The rationale behind this approach was to find an easy to use, relative (non-calibrated) equivalent for the so-called Tasseled Cap (TC) approach that has been developed for multispectral satellite data such as Landsat, resulting in equivalent brightness, greenness and yellowness components, with the difference that the TC components require customized coefficients that are not the same as the coefficients automatically generated by a PCA. Once the components mainly corresponding to brightness and greenness were identified, the brightness map was classified using a non-supervised isocluster algorithm with 5 classes to identify and mask shadow areas.

To investigate the relationship between the different VVI values derived from the orthomosaics with the Trimble GreenSeeker measurements, some preprocessing steps were implemented. First, a 16 cm radius buffer was generated around the GNSS measured GreenSeeker points. Next, UX5-based VVI pixel values within the buffer were averaged 5 x 5 to a 15 cm grid for extraction. After extraction, the 15cm pixel values belonging to the same buffer were again averaged to match the footprint of the imagery-based VVI values to the single averaged GreenSeeker readings.

For a specific field, the relation of VVI values to soil characteristics was investigated based on the bare earth digital elevation model (DEM) generated during image processing of the 19 Mar. 2014 dataset on the one hand, and the best performing VVI map of the 28 May 2014 dataset on the other hand (fig. 2B and 5A).

Table 1. Vegetation vigor indices (VVI) calculated at 3 cm GSD based on the processed UAS datasets.

Date	Bands	VVI	Remarks
19 Mar. 2014	RGNIR	NDVI	$(b3 - b1) / (b3 + b1)$
		GNDVI	$(b3 - b2) / (b3 + b2)$
		TSAVI	$\frac{s \times (b3 - s \times b1 - a)}{a \times b3 + b1 - a \times s + 0.18 \times (1 + s^2)}$ with a = intercept and s = slope of the *b3*/*b1* bare soil line
		PCA-2	2nd component of Principal Components Analysis using *b1*, *b2* and *b3* as input
28 May 2014	RGNIR	NDVI	same as above
		GDNVI	same as above
		TSAVI	same as above
		PCA-1	1st component of Principal Components Analysis using *b1*, *b2* and *b3* as input
	NIRG	GNDVI	$(b1 - b2) / (b1 + b2)$
		GTSAVI	$\frac{s \times (b1 - s \times b2 - a)}{a \times b1 + b2 - a \times s + 0.18 \times (1 + s^2)}$
		PCA-1	1st component of Principal Components Analysis using *b1* and *b2* as input

In order to mitigate the influences of field management patterns such as planting furrows that were not present in the first dataset, both datasets were downsampled to a 3 m grid prior to data extraction.

RESULTS AND DISCUSSION

Based on RTK GNSS-measured independent check points not used during image processing, the average horizontal root mean squared error (RMSE) for all datasets was 3.2 (± 0.3) cm while the average vertical RMSE for all datasets was 3.5 (± 0.4) cm, proving the pixel-level alignment accuracy necessary to perform multitemporal analyses or multiband calculations based on two orthomosaics.

Visual interpretation of the true and false color orthomosaics shown in fig. 2 and 3 already revealed important patterns and contrast differences in some band combinations that cannot be seen in others, most notably in discerning the earliest growth stages of crops on bare soil.

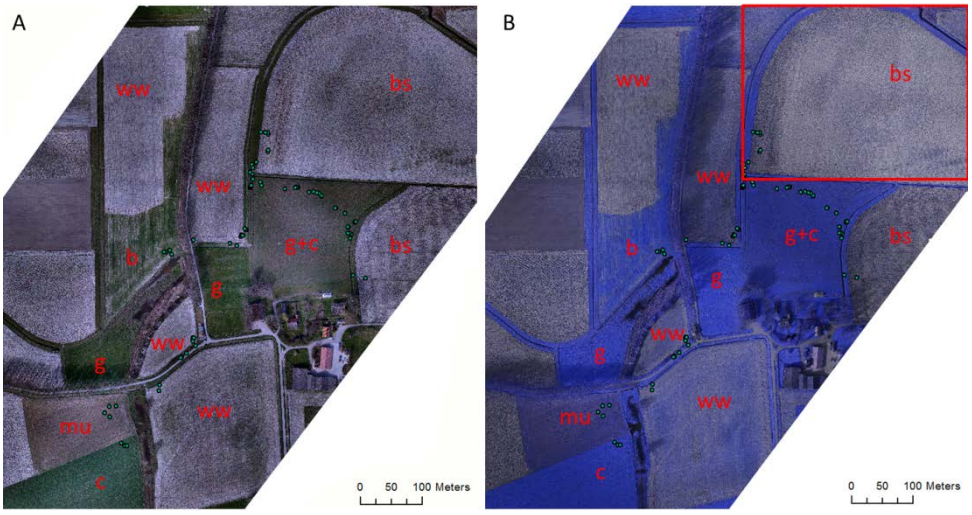

Figure 2. Orthomosaics of the 19 Mar. 2014 flights. **A:** R(b1):G(b2):B(b3) using the 486 UV/NIR blocking filter. **B:** R(b1):G(b2):NIR(b3) using the 040 orange filter. The red box in the NE corner of the RGNIR orthomosaic indicates the location of the DEM shown in fig. 6. The green dots indicate the 75 locations of Trimble GreenSeeker measurements. c = clover; b = barley (Feekes growth stage 4); bs = bare soil; g = grass; mu = mustard (senesced); ww = winter wheat (Feekes growth stages 1-3).

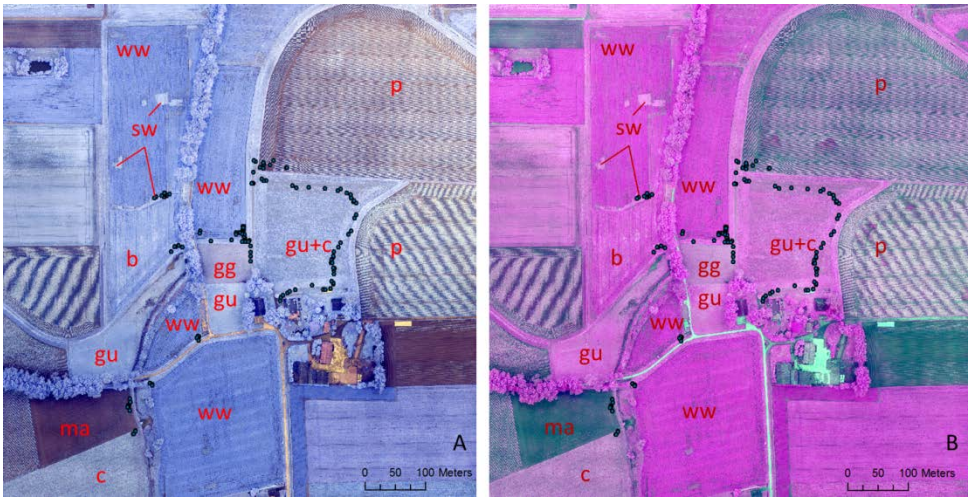

Figure 3. Orthomosaics of the 28 May 2014 flights. **A:** R(b1):G(b2):NIR(b3) using the 040 orange filter. **B:** NIR(b1):G(b2) using the 062 green filter. Brightness and contrast differences between fig. 2B and fig. 3A are primarily due to a different histogram stretching. Diagonal banding in some fields is due to moiré occurring on row crops when zoomed out, disappearing when zooming in to the plant level, revealing the actual crop rows. The dots indicate the 120 locations of Trimble GreenSeeker measurements. c = clover; b = barley (Feekes growth stage 10.5); gg = grass grazed; gu = grass ungrazed; ma = maize (VE growth stage); p = potato (growth stage II-III); sw = summer wheat (Feekes growth stage 4), ww = winter wheat (Feekes growth stages 8-10).

Even so, the calculation of VVI maps revealed more contrasts and additional properties on these earliest growth stages that were not visually apparent from the false color orthomosaics (fig. 4 and 5). For the 19 Mar. 2014 RGNIR dataset, the NDVI already showed meaningful patterns, with a linear fit (r) of 0.78 to GreenSeeker measurements (table 2). However, both the NDVI and GNDVI were clearly affected by shadows cast by buildings, trees, and even small terrain elevation changes and herbaceous vegetation, with coincidentally few GreenSeeker measurement points falling within shadow areas (fig. 4D).

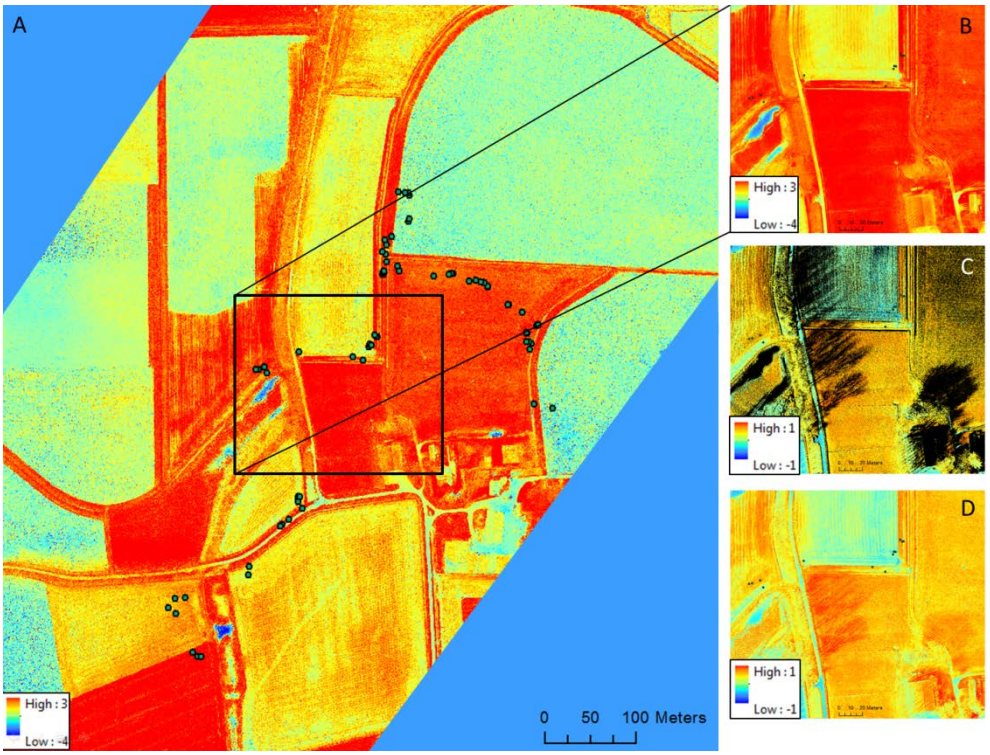

Figure 4. A: The 19 Mar. 2014 VVI map with the highest correlation to Trimble GreenSeeker measurements: TSAVI. While distinguishing wet bare soil in the NE field from emerging winter wheat in Feekes growth stage 3 in the central south field was impossible on fig. 2A (RGB), and while distinguishing dry bare soil in the NE field from emerging winter wheat in Feekes growth stage 1 on the same soil type in the NW field was also almost impossible on fig. 2B (RGNIR), the contrasts are very clearly visible in this TSAVI map. **B:** Selected area from the TSAVI map, where large shadows barely influence the VVI values. **C:** Same area as fig. 4B, showing the NDVI superimposed with the 1st cluster from the isocluster unsupervised classification of the 1st principal component (brightness) of the PCA based on the RGNIR orthomosaic, shown in black. Note how pixels affected by large tree shadows as well as small shadows caused by microrelief in the terrain and herbaceous vegetation are accurately identified. **D:** Same area as fig. 4B and 4C, showing the NDVI only. Note how shadow areas identified in fig. 4C are affected by artificially high NDVI values.

The PCA based on RGNIR data from 19 Mar. 2014 resulted in 2 immediately meaningful components, with the 1st component representative of brightness and the 2nd component corresponding to greenness. While the greenness component performed only slightly below the TSAVI (show in fig. 4A) in relation to GreenSeeker measurements, the 1st isocluster class obtained from the brightness component accurately identified all shadow (and water) areas in the image (fig. 4C). This layer could potentially be used to mask out all shadow areas within the NDVI map for interpretation, and it is conceivable that the 1st component could be used to modify the NDVI to mitigate brightness fluctuations from the beginning.

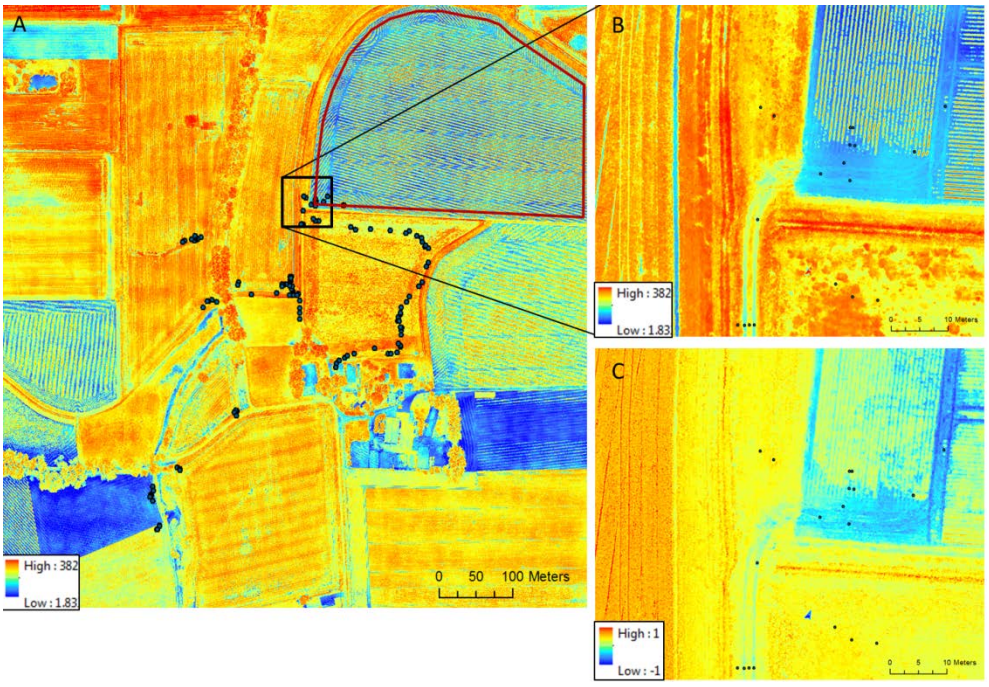

Figure 5. A: The 28 May 2014 VVI map with the highest correlation to Trimble GreenSeeker measurements: PCA-1 based on the NIRG dataset. The red line around the NE field shows the extent of the PCA-1 map that was used to correlate the VVI values to the DEM obtained from the 19 Mar. 2014 RGNIR dataset (see also fig. 2B). **B:** zoomed area of the NIRG-based PCA-1 map. Note how in the NE field potato plants on the furrow ridges and some weeds in between the rows are clearly visible, in sharp contrast to the bare soil of the furrows in between the rows. Note also how tractor tracks and the ditch running north to south in the western part of the image are clearly visible as showing low VVI values. In the SE part of the image, green clover patches can be clearly distinguished in the dry grass field. **C:** same area as in fig. 5B, showing the 28 May 2014 VVI map with the lowest correlation to Trimble GreenSeeker measurements: NDVI based on the RGNIR dataset. Note the large amount of soil noise in between potato rows and plants, and the ditch and tractor tracks showing abnormally high NDVI values. Also, the green clover patches in the dry grass field are very hard to discern.

Next to shadow issues in the NDVI map of the 19 Mar. 2014 RGNIR dataset, it was also impossible to find a hard threshold separating bare soil from fields with very sparse vegetative cover in the earliest growth stages based on the NDVI. Although the greenness component of the PCA did allow for a clear separation, contrasts were further amplified by the TSAVI, which had the added advantage of noticeably mitigating shadow areas as well (fig. 4A and 4B). However, due to few GreenSeeker measurements in shadow areas, it is yet unclear to what extent shadows are effectively removed in the TSAVI, and whether this can be generalized to other datasets as well.

In contrast to the 19 Mar. 2014 dataset, VVI maps based on the RGNIR dataset of 28 May 2014 correlated very poorly (if at all) to GreenSeeker measurements (table 2). Even in the absence of direct sunlight and hence strong shadows, both the NDVI and GNDVI artificially highlighted small open spaces in vegetation canopies, such as tractor tracks and ditches, with the highest NDVI values typically around rather than on individual plants (fig. 5C). Soil noise was also significant, to the extent that crop rows and emerging vegetation could not be separated from bare soil, and isolated green plants were barely distinguished from surrounding dry, short grass cover. Remarkably, as opposed to the 19 March dataset, soil-adjusted VVI maps based on the RGNIR dataset did not perform much better.

On the other hand, VVI maps based on the NIRG imagery for the same date did yield remarkably better correspondence with GreenSeeker measurements (table 2), especially soil-adjusted VVI maps and specifically the 1st principal component, in this case corresponding to greenness (fig. 5A), which allowed excellent separation between bare soil and emerging vegetation and crop rows, while accurately discriminating open spaces in the crop canopy such as from tractor tracks (fig. 5B).

Table 2. Linear relation coefficients of the different UAS-based vegetation vigor indices (VVI) with GreenSeeker measurements. The strongest relationship for each date is shown in bold.

Date	Bands	VVI	R
19 Mar. 2014	RGNIR	NDVI	0.74
		GNDVI	0.66
		TSAVI	**0.83**
		PCA-2	0.81
28 May 2014	RGNIR	NDVI	0.04
		GDNVI	0.16
		TSAVI	0.17
		PCA-1	0.12
	NIRG	GNDVI	0.45
		GTSAVI	0.79
		PCA-1	**0.83**

It is yet unknown what caused the remarkably low correlations of the VVI maps based on RGNIR imagery on 28 May 2014 in comparison with the NIRG data from that same day on the one hand, and the good results from RGNIR data on 19 Mar. 2014 on the other hand. A part of the explanation may be found in the presence of water on leaves and the (much darker) humid soil due to the light rain on 28 May, which may have been better accounted for by the elimination of out-of-band RE radiation with the 062 green filter. However, it is unknown how the 062 green filter would have performed in getting NIRG imagery and producing VVI maps in the 19 Mar. 2014 conditions, as that filter was not yet available on the first flight day and we have not yet had any opportunities to use the filter in similar conditions since. Specifically for the TSAVI, the performance differences can be partly explained by the obvious difference in total irradiance, as JPEG DNs were used while all soil-adjusted vegetation vigor indices normally require the use of reflectance factors. Another effect of irradiance differences between both dates can be seen in the PCA, where for the RGNIR as well as the NIRG analysis of 28 May, the 1st rather than the 2nd component represented greenness, while the 2nd component related to brightness (as opposed to the 19 March analyses).

In relating aerial VVI maps to ground-based GreenSeeker NDVI values, we want to point out that GreenSeeker NDVI readings are related to conditions in the upper parts of a vegetation canopy only, due to the fact that the GreenSeeker is an active optical system that uses a source of visible light and NIR close to the canopy. Both the spectral irradiance of this source, and the reflected radiation, decrease with distance, in accordance with the inverse square law. Therefore, the vast majority of reflected radiant energy being sensed by the GreenSeeker is for the part of the canopy that is closest to the sensor. By contrast, the reflected NIR radiation in aerial imagery comes from the entire canopy. So, it is possible that the GreenSeeker NDVI data differ from aerial imagery-related VVI data just due to how leaves may differ between the top of the canopy and the lower parts.

Although we were primarily looking for linear relationships between VVI maps and GreenSeeker measurements, logarithmic regressions have also been tested in preliminary analyses. Also, it was investigated whether combining RGB and RGNIR orthomosaics from two flights on the same day in the calculation of VVI maps (with visible color bands taken from the RGB imagery in order to get spectral signals unaffected by out-of-band radiation) would improve the correlations. While r results based on logarithmic regression and RGB-RGNIR combined datasets could typically deviate by ± 0.05 from linear r values based on single orthomosaic-derived VVI maps, fundamental trends did not change at all.

As the GreenSeeker NDVI measurements are known to saturate on dense vegetation canopies while some imagery-based vegetation vigor indices are theoretically less sensitive to saturation, we also inspected the graphs for any signs of saturation which would result in VVI points to bend upwards from a certain GreenSeeker NDVI level. However, we did not find any signs of saturation in one type of measurement that did not occur in the other.

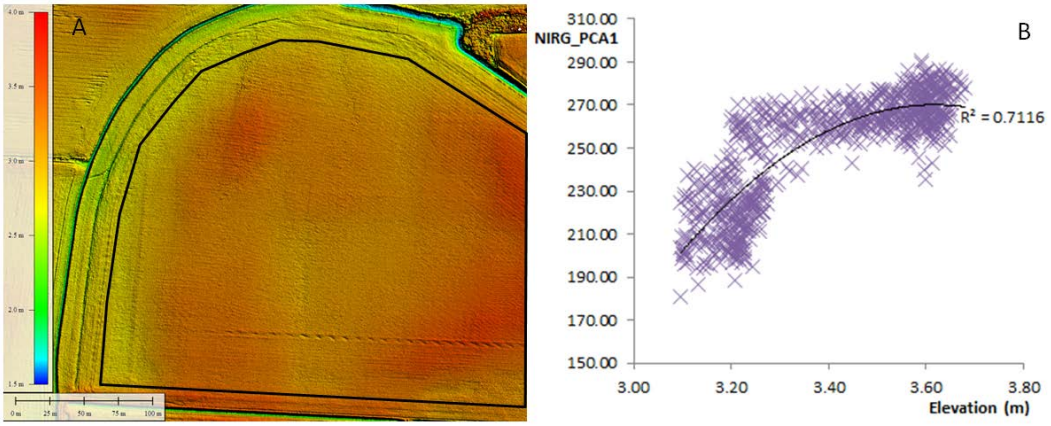

Figure 6. A: 6cm DEM obtained from the 19 Mar. 2014 RGNIR dataset, after plowing but before potato planting furrows had been created. A central depression can be seen, where the clay density is historically higher than the surroundings. The elevation difference between the lowest part in the central depression and the highest points surrounding the depression are in the order of 0.5m. **B:** Analysis showing the relation between potato NIRG-based PCA-1 VVI values on 28 May 2014 as obtained from the area delineated in red in fig. 5A, and elevation as derived from fig. 6A. The predictive nature of the soil (and hence the elevation) patterns on vegetation vigor can be best approached by a 2nd degree polynomial function (r = 0.71).

The maximum obtained r values in this study are very comparable to what other studies have found based on Trimble UX5 and Trimble Gatewing X100-derived, out-of-camera JPEG-based VVI maps related to ground-based vegetation measurements, at least when considering other vegetation vigor indices than the NDVI, potentially using other band combinations using different filters (e.g. Melchiori et al., 2014). Although these r values demonstrate that meaningful patterns can be inferred from the imagery, some gaps and outliers remain.

To our knowledge, there are no studies getting better correlations with physical, ground-measured vegetation parameters based on out-of-camera JPEG processing, illustrating the need for calibrated algorithms based on uncompressed, linear RAW data processing to get more precise VVI maps as a basis for quantitative input calculations such as prescriptions maps for variable rate application. Also, it must be noted that, while providing good correlations with Trimble GreenSeeker measurements on any one day, even the best VVI maps in this study did not show any consistency over time. For instance, thistles that clearly showed an increase in vigor from the first flight to the next, with GreenSeeker NDVI values increasing from 0.80 to 0.86, showed decreasing TSAVI values from 0.017 to 0.009 over time. This is illustrative of relative, uncalibrated VVI maps due to working on compressed, distorted JPEG DNs rather than reflectance factors or otherwise calibrated signals. Hence, these relative VVI maps can provide valuable insights for crop scouting on any single day, but cannot be interpreted in a multitemporal context without applying calibration algorithms on linear uncompressed RAW data.

Besides GreenSeeker measurements, an attempt was also made to correlate VVI values to other variables such as soil characteristics. Due to a lack of ancillary soil data, a correlation analysis was based on elevation, which, for one specific field, was known to be determined by clay density (with compaction levels being higher in the central depression than on the surrounding elevated parts). The height difference between the central depression and the elevated surroundings is hardly, if at all, noticeable in the field, but in wet winters, the central depression is often flooded by rain. Starting from a bare soil elevation model before furrow management and planting on 19 Mar. 2014, values of the downsampled greenness component of the NIRG dataset on 28 May were clearly, though not linearly, determined by the soil pattern ($r = 0.71$). This predictive effect of elevation (and hence compaction levels) on vegetation vigor two months later, regardless of furrow management activities that partly, but not entirely obscured the elevation differences, was not apparent from any of the RGNIR vegetation vigor maps or the GNDVI based on NIRG data on 28 May ($-0.14 < r < 0.42$).

Overall, these results highlight the need for flexible band combinations through the use of different external filters, enabling the calculation of VVI maps that are more robust to influences of irradiance and soil, in order to enable reliable crop scouting based on processing out-of-camera JPEG imagery from modified commercial cameras onboard UAS.

CONCLUSION AND PERSPECTIVES

While the general applicability of the alternative approaches discussed in the paper remain to be tested for rigidity across all scenarios, high correlations of aerial orthomosaic-based VVI maps with Trimble GreenSeeker NDVI values can be achieved. This demonstrates that UAS-based crop scouting using out-of-camera JPEG imagery and readily available image processing techniques is very promising. At the same time, the results highlight the fact that although a simple NDVI using this approach may sometimes reveal meaningful patterns, there is a significant risk of inferring invalid conclusions related to crop vigor, depending on the conditions, when relying only on the NDVI. The ability to work with multiple external filters on the Trimble UX5 in order to get different band combinations and work with alternative vegetation vigor indices, as opposed to relying only on the image-based NDVI, appears to be crucial for reliable crop scouting, greatly improving correlations with accepted quantitative ground-based crop scouting techniques. Even so, more precise data for multitemporal analysis and quantitative prescription mapping for variable rate application can only be gathered by applying calibrated algorithms to uncompressed linear RAW data.

ACKNOWLEDGEMENTS

Jack Paris (Trimble Navigation and Paris Geospatial LLC, Clovis, CA), and Jerome Coonen, Arthur Lange, and Jim Quaderer (Trimble Ag Imaging R&D group, Sunnyvale, CA) provided elaborate feedback during discussions of the present work. Marc De Schepper is acknowledged for enabling ground measurements and UAS flights and for sharing farm management data on his fields discussed in this study.

REFERENCES

Hunt, R.E.Jr., Hively, W.D., Fujikawa, S.J, Linden, D.S., Daughtry, C.S.T., and McCarty, G.W. 2010. Acquisition of NIR-Green-Blue digital photographs from unmanned aircraft for crop monitoring. Remote Sensing 2: 290-305.

Lebourgeois, V., Bégué, A., Labbé, S., Houlès, M., and Martiné , J.F. 2012. A light-weight multi-spectral aerial imaging system for nitrogen crop monitoring. Precision Agriculture 13: 525-541.

Lebourgeois, V., Bégué, A., Labbé, S., Mallavan, B., Prévot, L., and Roux, B. 2008. Can commercial digital cameras be used as multispectral sensors? A crop monitoring test. Sensors 8: 7300-7322.

Lelong, C.C.D., Burger, P., Jubelin, G., Roux, B., Labbé, S., and Baret, F. 2008. Assessment of unmanned aerial vehicles imagery for quantitative monitoring of wheat crop in small plots. Sensors 8: 3557-3585.

Melchiori, R.J.M., Kemerer, A.C., and Albarenque, S.M. 2014. Unmanned aerial system to determine nitrogen status in maize. Proceedings of the INTA National Congress of Precision Agriculture 2014 (Argentina): 13pp.

Mulla, D.J. 2013. Twenty five years of remote sensing in precision agriculture: key advances and remaining knowledge gaps. Biosystems Engineering 114: 358-371.

West, G. 2014. Unmanned systems and agriculture: an industry on the rise. Oral presentation at The InfoAg Conference, 29-31 July 2014, St. Louis, MO, USA.

Zhang, C., and Kovacs, J.M. 2012. The application of small unmanned aerial systems for precision agriculture: a review. Precision agriculture 13: 693-712.